On the Noise Enhancement of GFDM

Mohammad Towliat, Morteza Rajabzadeh, and Seyyed Mohammad Javad Asgari Tabatabaee

***Abstract*—Generalized frequency division multiplexing (GFDM) is a multicarrier system employing well-localized prototype filters to form the transmitted signal. However, because of the non-orthogonality of the waveform, the demodulation process of GFDM inherits a noise enhancement, which leads to the performance degradation. Eigenvalues of the GFDM matrix determine the level of noise enhancement. In this paper, by defining the condition number of the GFDM matrix as the noise enhancement factor (NEF), we derive a closed-form presentation of NEF criterion based on the prototype filter shape. We show that the value of NEF is independent of the number of subsymbols and subchannels, if they are even; contrarily, for odd numbers, a larger NEF is resulted as the number grows up.**

***Index Terms*—Condition number, GFDM matrix, Noise enhancement**

I. Introduction

Generalized frequency division multiplexing (GFDM) has been introduced as a replacement for orthogonal frequency division multiplexing (OFDM) in future networks [1]. In GFDM, the high out-of-band emission problem of OFDM is tackled by shaping the transmitted signal with spectral well-localized filters [2]. In general, the complexity of GFDM implementation is more than that of OFDM; however, in some works, low latency and simplified versions of GFDM are developed [3]. Despite all advantages, the demodulation of GFDM involves a noise enhancement which leads to degradation of the bit error rate (BER) performance. Noise enhancement is a result of the non-orthogonal nature of GFDM and tightly depends on the configuration of the prototype filter. This dependency is such that in some cases the implementation of GFDM becomes infeasible [4]. In this paper, we investigate the noise enhancement source by extracting the eigenvalues of the GFDM matrix and define the noise enhancement factor (NEF) based on the dispersion of these eigenvalues. We show how the number of subsymbols and subchannels in GFDM determine the eigenvalues, and eventually, impact the NEF. The rest of this paper is organized as follows. In Section II, the system model of GFDM is presented. Section III describes the NEF and its relation to the GFDM parameters. Finally, Section IV concludes the paper.

II. System Model

In a GFDM system with K subsymbols and L subchannels, by defining $N = KL$, the modulator's output vector is given as $\mathbf{s} = \mathbf{A}\mathbf{d}$, where $\mathbf{s} \in \mathbb{C}^{N\times 1}$ is the GFDM modulator's output vector and $\mathbf{d} \in \mathbb{C}^{N\times 1}$ is the vector of data symbols. $\mathbf{A} = [\mathbf{G}_0, \mathbf{G}_1, \dots \mathbf{G}_{K-1}] \in \mathbb{C}^{N\times N}$ is also known as the GFDM matrix, in which the (m,l)th entry of $\mathbf{G}_k \in \mathbb{C}^{N\times L}$ (for $k = 0, \dots K-1$) is given as [5]

$$[\mathbf{G}_k]_{m,l} = g[(m-kL)_N]\, e^{j2\pi ml/L}. \tag{1}$$

where $(.)_N$ denotes the modulo of N. Passing through the channel, the received signal vector yields to [6]

$$\mathbf{y} = \mathbf{H}\mathbf{s} + \mathbf{w} = \mathbf{H}\mathbf{A}\mathbf{d} + \mathbf{w}, \tag{2}$$

where $\mathbf{H} \in \mathbb{C}^{N\times N}$ denotes the circular matrix of the channel impulse response and $\mathbf{w}$ is the additive noise vector with the power of N_0. In order to estimate data symbol vector $\mathbf{d}$, the zero forcing (ZF) matrix $(\mathbf{H}\mathbf{A})^{-1}$ is applied to the received vector, such that

$$\hat{\mathbf{d}} = (\mathbf{H}\mathbf{A})^{-1}\mathbf{y} = \mathbf{d} + (\mathbf{H}\mathbf{A})^{-1}\mathbf{w}, \tag{3}$$

where $\hat{\mathbf{d}}$ denotes the estimated symbol vector.

III. GFDM Output Noise

A. NEF Definition

According to (3), the final noise vector contaminating the estimated data symbols is $(\mathbf{H}\mathbf{A})^{-1}\mathbf{w}$. Obviously, GFDM matrix $\mathbf{A}$ impacts the output noise, and consequently, affects the bit error probability (BEP) at the detection process. In order to investigate the effect of $\mathbf{A}$ on the noise, without loss of generality, let us suppose that the channel is AWGN. With this respect, the BEP of GFDM becomes [3]

$$p_b \approx \frac{2(\sqrt{\mathcal{M}}-1)}{\sqrt{\mathcal{M}}\log_2(\mathcal{M})}\mathrm{erfc}\left(\sqrt{\frac{3\log_2(\mathcal{M})}{2(\mathcal{M}-1)} \times \frac{E_b}{\xi N_0}}\right), \tag{4}$$

where E_b is the average energy per bit in the $\mathcal{M}$-QAM constellation and $\xi = \frac{1}{N}\sum_{i=0}^{N-1} {}^1\!/_{\lambda_i}$, in which λ_i, for $i = 0, \dots N-1$, denote the eigenvalues of $\mathbf{\Psi} = \mathbf{A}^H\mathbf{A}$. According to (4), ξ (the average of ${}^1\!/_{\lambda_i}$'s) is acting as a noise power multiplier in BEP. Therefore, in some works (e.g. [2]), ξ is used as a criterion to determine the noise enhancement in GFDM. However, investigating the value of ξ is not straightforward.

Nevertheless, recall from (1) that the entries of $\mathbf{A}$ depend on the prototype filter $g[m]$. Since $g[m]$ has a normalized power shape, we have always $\frac{1}{N}\|\mathbf{A}\|_2^2 = 1$, which indicates that $\frac{1}{N}\sum_{i=0}^{N-1}\lambda_i = 1$. In other words, regardless of the prototype filter's shape, the average of λ_i's is always fixed to the unit value. Thus, one can conclude that p_b is mainly determined by those small eigenvalues which are $\lambda_i < 1$, and the other eigenvalues have a negligible effect. In this regard, to simply investigate the effect of the filter's shape on the output noise,

M. Towliat is with the Department of Electrical and Computer Engineering, University of Delaware, DE, USA, (e-mail: mtowliat@udel.edu). M. Rajabzadeh is with the Department of Electrical Engineering, Quchan University of Technology, Quchan, Khorasan Razavi, Iran (e-mail: m.rajabzadeh@qiet.ac.ir). S. M. J. Asgari Tabatabaee is with the Department of Electrical and Computer Engineering, University of Torbat Heydarieh, Torbat Heydarieh, Iran (e-mail: s.m.j.asgaritabatabaee@torbath.ac.ir).

This article has been accepted for publication in a future issue of this journal, but has not been fully edited. Content may change prior to final publication. Citation information: DOI 10.1109/LWC.2020.2983367, IEEE Wireless Communications Letters

we define the condition number of $\mathbf{\Psi}$ as the noise enhancement factor (NEF) in GFDM. Condition number is a measure of eigenvalues dispersion and is given as

$$\chi = \frac{\lambda_{\max}}{\lambda_{\min}}, \tag{5}$$

where $\lambda_{\max} = \max_i \{\lambda_i\}$ and $\lambda_{\min} = \min_i \{\lambda_i\}$. According to the discussion above, the NEF criterion in (5) is important and must be taken into account, for the purpose of comparing and designing GFDM prototype filters.

B. Calculating the Eigenvalues

The first step to investigate the NEF in (5) is to obtain the eigenvalues of $\mathbf{\Psi}$ for a given filter $g[m]$. Before doing that, let us have a look at the structure of matrix $\mathbf{\Psi}$.

If we consider that, for $k_1, k_2 = 0, \dots K-1$, $\mathbf{\Psi}^{(k_1,k_2)} \in \mathbb{C}^{L\times L}$ is the (k_1,k_2)th submatrix of $\mathbf{\Psi} \in \mathbb{C}^{N\times N}$, from the definition of $\mathbf{A}$, one can see that $\mathbf{\Psi}^{(k_1,k_2)} = \mathbf{G}_{k_1}^H \mathbf{G}_{k_2}$. Thus, according to (1), for $l_1, l_2 = 0, \dots L-1$, the (l_1,l_2)th entry of $\mathbf{\Psi}^{(k_1,k_2)}$ becomes

$$\psi_{(l_1,l_2)}^{(k_1,k_2)} = \sum_{m=0}^{N-1} g[m] g[(m+\Delta k\, L)_N]\, e^{-j2\pi m\, \Delta l/L}, \tag{6}$$

where $\Delta k = k_1 - k_2$ and $\Delta l = l_1 - l_2$. As (6) shows, the value of $\psi_{(l_1,l_2)}^{(k_1,k_2)}$ just depends on Δk and Δl. Thus, for more facility, we abuse the notations and present $\psi_{(l_1,l_2)}^{(k_1,k_2)}$ with $\psi_{(\Delta l)}^{(\Delta k)}$ and indicate $\mathbf{\Psi}^{(k_1,k_2)}$ with $\mathbf{\Psi}^{(\Delta k)}$ at the rest of this paper.

On the other hand, since the prototype filter $g[m]$ has a symmetric shape in time and frequency, and satisfies the orthogonality condition [5], it is concluded that $\psi_{(\Delta l)}^{(\Delta k)}$ is also a real and symmetric function in both time and frequency domains, so that $\psi_{(\Delta l)}^{(\Delta k)} = \psi_{(\Delta l)}^{(-\Delta k)} = \psi_{(-\Delta l)}^{(\Delta k)}$. Considering the time symmetry (i.e. $\psi_{(\Delta l)}^{(\Delta k)} = \psi_{(\Delta l)}^{(-\Delta k)}$), it is obtained that $\mathbf{\Psi}^{(\Delta k)} = \mathbf{\Psi}^{(-\Delta k)}$. In this regard, since $\mathbf{\Psi}^{(\Delta k)}$ is a submatrix of $\mathbf{\Psi}$, it is concluded that $\mathbf{\Psi}$ has the following block circular structure

$$\mathbf{\Psi} = \begin{bmatrix} \mathbf{\Psi}^{(0)} & \mathbf{\Psi}^{(1)} & \dots & \mathbf{\Psi}^{(K-1)} \\ \mathbf{\Psi}^{(1)} & \mathbf{\Psi}^{(0)} & \searrow & \vdots \\ \vdots & \searrow & \searrow & \mathbf{\Psi}^{(1)} \\ \mathbf{\Psi}^{(K-1)} & \dots & \mathbf{\Psi}^{(1)} & \mathbf{\Psi}^{(0)} \end{bmatrix}. \tag{7}$$

Furthermore, regarding the frequency symmetry (i.e. $\psi_{(\Delta l)}^{(\Delta k)} = \psi_{(-\Delta l)}^{(\Delta k)}$) and the fact that $\psi_{(\Delta l)}^{(\Delta k)}$ is the (l_1,l_2)th entry of $\mathbf{\Psi}^{(\Delta k)}$, one can see that in (7), each of $\mathbf{\Psi}^{(\Delta k)}$ for $\Delta k = 0, \dots K-1$, also has a circular structure such that

$$\mathbf{\Psi}^{(\Delta k)} = \begin{bmatrix} \psi_{(0)}^{(\Delta k)} & \psi_{(1)}^{(\Delta k)} & \dots & \psi_{(L-1)}^{(\Delta k)} \\ \psi_{(1)}^{(\Delta k)} & \psi_{(0)}^{(\Delta k)} & \searrow & \vdots \\ \vdots & \searrow & \searrow & \psi_{(1)}^{(\Delta k)} \\ \psi_{(L-1)}^{(\Delta k)} & \dots & \psi_{(1)}^{(\Delta k)} & \psi_{(0)}^{(\Delta k)} \end{bmatrix}. \tag{8}$$

By considering (7) and (8), it is clear that $\mathbf{\Psi}$ is a block circular matrix with circular submatrices nested in.

Now, let us obtain the eigenvalue decomposition (EVD) of $\mathbf{\Psi}$. To this end, we start with the EVD of $\mathbf{\Psi}^{(\Delta k)}$. Since $\mathbf{\Psi}^{(\Delta k)}$ is a circular matrix, its EVD is given as [7]

$$\mathbf{\Psi}^{(\Delta k)} = \mathbf{F}_L\, \mathbf{\Omega}^{(\Delta k)}\, \mathbf{F}_L^H, \tag{9}$$

where $\mathbf{F}_L$ is the L-point DFT matrix and $\mathbf{\Omega}^{(\Delta k)}$ is a diagonal matrix holding the eigenvalues of $\mathbf{\Psi}^{(\Delta k)}$, in which the uth diagonal entry is

$$\Omega_{(u)}^{(\Delta k)} = \sum_{\Delta l=0}^{L-1} \psi_{(\Delta l)}^{(\Delta k)}\, e^{-j2\pi\, u\, \Delta l\, /L}. \tag{10}$$

By replacing (9) in (7), we can represent $\mathbf{\Psi}$ as

$$\mathbf{\Psi} = (\mathbf{I}_K \otimes \mathbf{F}_L) \underbrace{\begin{bmatrix} \mathbf{\Omega}^{(0)} & \mathbf{\Omega}^{(1)} & \dots & \mathbf{\Omega}^{(K-1)} \\ \mathbf{\Omega}^{(1)} & \mathbf{\Omega}^{(0)} & \searrow & \vdots \\ \vdots & \searrow & \searrow & \mathbf{\Omega}^{(1)} \\ \mathbf{\Omega}^{(K-1)} & \dots & \mathbf{\Omega}^{(1)} & \mathbf{\Omega}^{(0)} \end{bmatrix}}_{\mathbf{\Omega}} \left(\mathbf{I}_K \otimes \mathbf{F}_L^H\right), \tag{11}$$

where $\otimes$ denotes the Kronecker product. From (11), it can be seen that $\mathbf{\Omega}$ is a block circular matrix constructed with diagonal submatrices $\mathbf{\Omega}^{(\Delta k)} \in \mathbb{C}^{L\times L}$. Thus, similar to what we did in (9), one can rewrite $\mathbf{\Omega}$ as

$$\mathbf{\Omega} = (\mathbf{F}_K \otimes \mathbf{I}_L) \underbrace{\begin{bmatrix} \mathbf{\Lambda}^{(0)} & & & \mathbf{0} \\ & \mathbf{\Lambda}^{(1)} & & \\ & & \ddots & \\ \mathbf{0} & & & \mathbf{\Lambda}^{(K-1)} \end{bmatrix}}_{\mathbf{\Lambda}} \left(\mathbf{F}_K^H \otimes \mathbf{I}_L\right), \tag{12}$$

where $\mathbf{F}_K$ is the K-point DFT matrix and $\mathbf{\Lambda}^{(v)} \in \mathbb{C}^{L\times L}$, for $v = 0, \dots K-1$, is a diagonal matrix with the uth entry equal to

$$\Lambda_{(u)}^{(v)} = \sum_{\Delta k=0}^{K-1} \Omega_{(u)}^{(\Delta k)}\, e^{-j2\pi v\, \Delta k/K}. \tag{13}$$

Finally, by substituting (12) in (11), EVD of $\mathbf{\Psi}$ is given as

$$\mathbf{\Psi} = (\mathbf{F}_K \otimes \mathbf{F}_L)\, \mathbf{\Lambda}\, \left(\mathbf{F}_K^H \otimes \mathbf{F}_L^H\right). \tag{14}$$

In (14), $\mathbf{F}_K \otimes \mathbf{F}_L$ is a unitary matrix and $\mathbf{\Lambda}$ is a diagonal matrix containing eigenvalues of $\mathbf{\Psi}$. Entries on the main diagonal of $\mathbf{\Lambda}$ are obtained by substituting (10) in (13) as

$$\Lambda_{(u)}^{(v)} = \sum_{\Delta k=0}^{K-1} \sum_{\Delta l=0}^{L-1} \psi_{(\Delta l)}^{(\Delta k)}\, e^{-j2\pi u\, \Delta l\, /L}\, e^{-j2\pi\, v\, \Delta k\, /K}. \tag{15}$$

Note that $\Lambda_{(u)}^{(v)}$ is the uth entry of $\mathbf{\Lambda}^{(v)}$, where $\mathbf{\Lambda}^{(v)}$ is the vth submatrix of $\mathbf{\Lambda}$ (for $u = 0, \dots L-1$ and $v = 0, \dots K-1$). In other words, for $i = 0, \dots N-1$, the ith eigenvalue of $\mathbf{\Psi}$ can be presented as

$$\lambda_i = \Lambda_{(u)}^{(v)};\ \ i = vL + u. \tag{16}$$

This article has been accepted for publication in a future issue of this journal, but has not been fully edited. Content may change prior to final publication. Citation information: DOI 10.1109/LWC.2020.2983367, IEEE Wireless Communications Letters

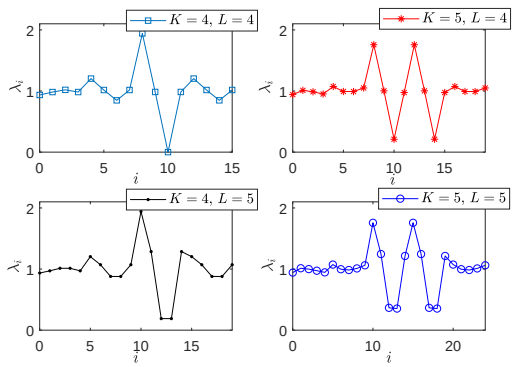

Fig. 1. Eigenvalues of the GFDM matrix for RRC pulse shape with $\alpha = 0.5$, when $(K, L) = (4, 4)$, $(4, 5)$, $(5, 4)$ and $(5, 5)$. Usually in practice, K is taken odd and L is set to an even number; however, to have a complete discussion, herein we covered all theoretically possible cases.

So far, we have inferred the eigenvalues of $\mathbf{\Psi}$ in (15) and (16). We can simplify this derivation by replacing (6) and (15) in (16), which yields to

$$\lambda_i = L\left|\sum_{k=0}^{K-1} g[(kL-u)_N]\, e^{-j2\pi vk/K}\right|^2 ;\ \ i = vL+u. \quad (17)$$

Eq. (17) is the simplified and closed-form presentation of eigenvalues of the GFDM matrix in terms of the prototype filter shape in the time domain, $g[m]$. It is noteworthy that to present the eigenvalues in terms of prototype filter in the frequency domain, one can use DFT properties [8], and represent (17) as $\lambda_i = \frac{1}{L}\left|\sum_{l=0}^{L-1} G[vL-lK]\ \exp(j2\pi ul/L)\right|^2$, where $G[n]$, for $n = 0, \dots N-1$, is the Fourier transform of $g[m]$. As an example of using (17), Fig. 1 illustrates λ_i's for the root raised cosine (RRC)[1] prototype filter with roll-off factor $\alpha = 0.5$. In this figure, (K, L) pair takes different values $(4, 4)$, $(4, 5)$, $(5, 4)$ and $(5, 5)$.

C. Calculating the NEF

In this section, we talk about obtaining the NEF in (5) by using the achieved eigenvalues in (17). To this purpose, recall that $g[m]$ is a real-valued and symmetric pulse shape. This fact leads to an interesting feature of eigenvalues in (17). That feature is that $\lambda_{\max}$ and $\lambda_{\min}$ can be simply acquired as

$$\begin{aligned} \lambda_{\max} &= \lambda_{v'L}, \\ \lambda_{\min} &= \lambda_{v'L+u'}, \end{aligned} \quad (18)$$

where

$$v' = \begin{cases} \frac{K}{2};\ \text{even } K \\ \\ \frac{K\pm1}{2};\ \text{odd } K \end{cases}, \quad u' = \begin{cases} \frac{L}{2};\ \text{even } L \\ \\ \frac{L\pm1}{2};\ \text{odd } L \end{cases}.$$

For instance, in Fig. 1, it can be seen that $\lambda_{\max}$ and $\lambda_{\min}$ take place as shown in (18). To have a better intuition of $\lambda_{\max}$ and $\lambda_{\min}$, for a given K and L, let us rewrite (17) as $\lambda_{vL+u} = \left|\sum_{k=0}^{K-1} f[kL-u]\ \exp(jh^{(v,u)}[kL-u])\right|^2$ in which $f[m] = L^2 g[m]$ and $h^{(v,u)}[m] = -2\pi v(m+u)/N$. By this consideration, nesting (18) in (5) leads to the NEF as

$$\chi = \frac{\left|\sum_{k=0}^{K-1} f[kL]\exp(jh^{(v',0)}[kL])\right|^2}{\left|\sum_{k=0}^{K-1} f[kL-u']\exp(jh^{(v',u')}[kL-u'])\right|^2}. \quad (19)$$

According to (19), Fig. 2 presents $f[KL]$, $f[kL-u']$, $h^{(v',0)}[kL]$ and $h^{(v',u')}[kL-u']$, for the given (K, L)'s in Fig. 1. As it can be seen, for the case where (K, L) is $(even, even)$ numbers, the involved components in $\lambda_{\min}$ cancel each other and we have always $\lambda_{\min} = 0$. In this case, $\mathbf{\Psi}$ is a singular matrix and the NEF in (19) becomes $\chi \to \infty$. This means that the output noise power is infinite and GFDM demodulation is infeasible. To address this concern, in some works, such as [9], the authors develop a method which shifts $f[m]$ or $h^{(v,u)}[m]$ to the left or right (see Fig. 2(a)), to avoid the singularity. However, according to Fig. 2, for the other cases (where (K, L) is not $(even, even)$) the singularity of $\mathbf{\Psi}$ does not occur. The plots in Fig. 1 also confirm these results. To elaborate the value of NEF when (K, L) is not $(even, even)$, in Fig. 3 we have plotted χ, given in (19). In Fig. 3(a), $K = 5$ and χ is calculated for different L's. As it can be seen, the NEF curve has up-and-down fluctuations, for even and odd values of L, such that for even L's, the NEF always remains constant (in this example $\chi \approx 8.5$); however, for odd L's it has a logarithmic escalation converging to the stable point (i.e. $\chi \approx 8.5$) as L increases. In addition, Fig. 3(b) illustrates the NEF for different K's, when $L = 31$ (note that although in practice, L usually takes even numbers, in this plot we choose odd L to make sure that the singularity never happens for any case study number of K). It is obvious that NEF in this figure also has up-and-down fluctuations for even and odd values of K, so that for even K's, NEF is always stable (in this example $\chi \approx 390$) and for odd K's, it has an exponential escalation as K increases. Besides, interestingly the steady trend of even K's meets the exponential trend of odd K's at the point where $K = L$ (in this example $K = 31$). These results are more sensible by looking at the plots in Fig. 2. All in all, the achievements in this section can be wrapped up as follows: in a GFDM system, each of K and L parameters can theoretically take even or odd numbers. If a parameter is even, in terms of NEF, it does not matter which even number that parameter takes. On the other hand, if a parameter is odd, the number set to that parameter affects the NEF, such that a larger odd K escalates NEF exponentially; while a larger odd L increases the NEF logarithmically.

Another point is that in this article, the NEF of GFDM is provided for the AWGN channel, where the noise is determined just by the GFDM matrix. Contrarily, in fading channels, the NEF not only depends on the GFDM matrix, but also tangles with the channel frequency response [2]. However, with a good approximation, the contribution of the GFDM matrix in NEF provided in this article, can be extended to that of fading channels. To verify this statement and the other

[1]In this paper, we studied the RRC filter, for instance. However, all provided derivations are applicable for any other orthogonal pulse shapes used in GFDM.

This article has been accepted for publication in a future issue of this journal, but has not been fully edited. Content may change prior to final publication. Citation information: DOI 10.1109/LWC.2020.2983367, IEEE Wireless Communications Letters

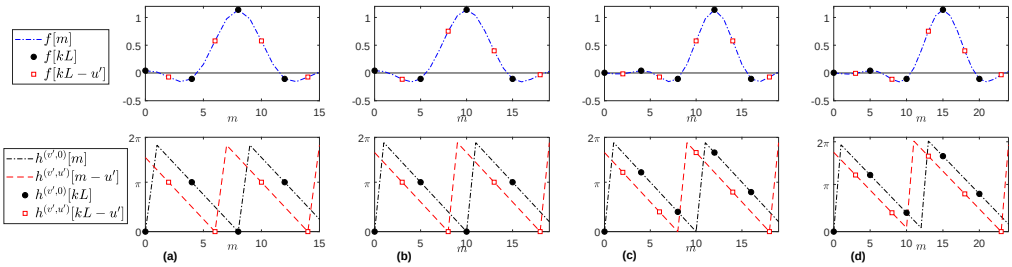

Fig. 2. Illustrating the involved values in $\lambda_{\max}$ and $\lambda_{\min}$, with dark circles and bright squares, respectively. The plots are given when (K, L) is (a) $(even, even)$, (b) $(even, odd)$, (c) $(odd, even)$, and (d) (odd, odd).

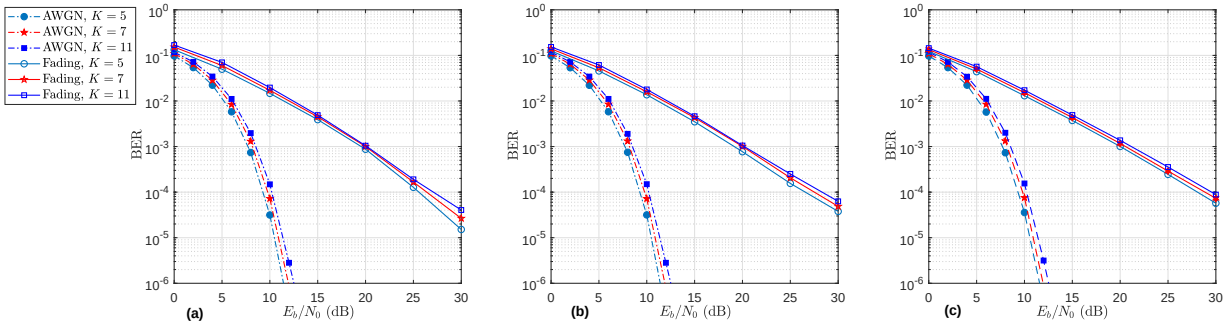

Fig. 4. The BER of GFDM using 4-QAM constellation and RRC filter with $\alpha = 0.5$ in AWGN and fading channels. It is considered that $K = 5, 11, 15$; when (a) $L = 32$, (b) $L = 64$, and (c) $L = 128$.

aforementioned achievements, Fig. 4 presents the BER results for the simulated GFDM in both AWGN and Vehicular-A fading channel, when $K = 5, 7, 11$; and $L = 32, 64, 128$. In the case of AWGN channel, by separately looking at each Fig. 4(a), Fig. 4(b) and Fig. 4(c), it is seen that while L is an even number, a higher BER is delivered for a larger odd K; however, by comparing Fig. 4(a), Fig. 4(b) and Fig. 4(c) together, one can see that for an odd K, by increasing the even L, the BER curves remain identical. These results confirm the achievements in Fig. 3. On the other hand, in Fig. 4 the same behavior is observed for the BER in the fading channel. The only difference is that in this case, BER slightly grows up as the even L increases, which is caused by the frequency selectivity of the channel.

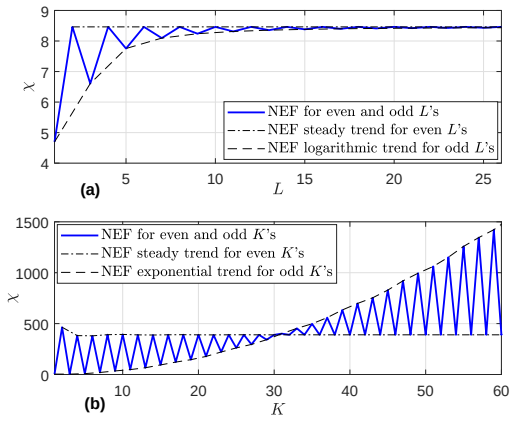

Fig. 3. The NEF of RRC filter with $\alpha = 0.5$, (a) for different L's, when $K = 5$, and (b) for different K's, when $L = 31$.

IV. Conclusions

In this article, we showed that the noise enhancement factor (NEF) of GFDM system can be defined as the condition number of the GFDM matrix. In order to calculate the NEF, we obtained the eigenvalues of GFDM matrix for a given prototype filter and then, we found a closed-form presentation for NEF. Based on that, we showed that by considering the number of subsymbols and subcarriers as two GFDM parameters, the NEF is independent of the value of the even parameter and increases as the value of the odd parameter grows up.

References

[1] G. Fettweis, M. Krondorf, and S. Bittner, "GFDM-generalized frequency division multiplexing," in *Proc. IEEE 69th Veh. Technol. Conf. (VTC)*. Barcelona, Spain, Apr. 2009, pp. 1–4.

[2] N. Michailow *et al.*, "Generalized frequency division multiplexing for 5th generation cellular networks," *IEEE Trans. Commun.*, vol. 62, no. 9, pp. 3045–3061, Sep. 2014.

[3] A. Farhang, N. Marchetti, and L. E. Doyle, "Low-complexity modem design for GFDM," *IEEE Trans. Signal Process.*, vol. 64, no. 6, pp. 1507–1518, Mar. 2016.

[4] D. W. Lin and P.-S. Wang, "On the configuration-dependent singularity of GFDM pulse-shaping filter banks," *IEEE Commun. Lett.*, vol. 20, no. 10, pp. 1975–1978, Oct. 2016.

[5] M. Towliat and S. M. J. A. Tabatabaee, "GFDM interference mitigation without noise enhancement," *IEEE Commun. Lett.*, vol. 22, no. 5, pp. 1042–1045, May. 2018.

[6] M. Towliat, S. M. J. A. Tabatabaee, and M. Rajabzadeh, "A simple ML detection for coded generalized frequency division multiplexing in MIMO channels," *IEEE Trans. Signal Process.*, vol. 67, no. 3, pp. 798–807, Feb. 2019.

[7] A. Goldsmith, *Wireless communications*. Cambridge university press, 2005.

[8] J. G. Proakis, *Digital signal processing: principles algorithms and applications*. Pearson Education India, 2001.

[9] A. Yoshizawa, R. Kimura, and R. Sawai, "A singularity-free GFDM modulation scheme with parametric shaping filter sampling," in *Proc. IEEE 84th Veh. Technol. Conf. (VTC-Fall)*, Montreal, QC, Mar. 2016, pp. 1–5.